Supporting Information

Gnanapragasam et al. 10.1073/pnas.1015341108

SI Methods

Protein Preparation. The coiled-coil regions of human methyl-binding domain 2b (MBD2b; amino acids 211–244) and p66α (amino acids *138–178*, *144–158*, *152–168*, or *144–168*; throughout, italics indicate p66α amino acids) were cloned and expressed as thioredoxin fusion proteins using a pET32a vector [modified to incorporate a thrombin cleavage site immediately N-terminal to the cloned sequence (1)], purified by nickel Sepharose affinity and size-exclusion chromatography, and combined at a 1:1 molar ratio; then the thioredoxin fusion was removed by thrombin digestion. The isotopically labeled (^{15}N, ^{13}C) p66α (or MBD2) coiled-coil domain was purified as a monomer or as a heterodimer with unlabeled MBD2 (or p66α, respectively) coiled-coil domain by ion-exchange chromatography (Mono S 5/50 GL; GE Healthcare), and buffer was exchanged into NMR buffer [10 mM sodium phosphate (pH 6.5), 0.01% sodium azide, 1 mM DTT, 10% $^{2}H_2O$, 0.5–1.5 mM protein].

Analytical Ultracentrifugation and Binding Analysis. The p66α and MBD2 coiled-coil domains with N-terminal thioredoxin fusions were analyzed by gel filtration chromatography (Superdex75 10/300; GE Healthcare) under physiologic conditions [20 mM Tris (pH 8.0), 150 mM NaCl, 2 mM β-mercaptoethanol]. Analytical ultracentrifugation analysis using an XL-I Analytical Ultracentrifuge (Beckman Coulter) was performed in the same buffer (50 μM protein), the sedimentation velocity was fit to a continuous size distribution [c(s)], and the effective molecular weight was determined using the SEDFIT software (sedfitsedphat.nibib.nih.gov). For analysis of surface plasmon resonance binding (Biacore T100) (2), the MBD2 coiled-coil thioredoxin fusion was coupled to a Sensor Chip CM5 (GE Healthcare) per the manufacturer's protocol, the p66α coiled-coil thioredoxin fusion was passed over the surface (at concentrations from 200–7 nM), and the resulting sensorgram was fit to a 1:1 binding model.

Circular dichroism spectra were collected on peptide samples (33.3 μg/mL total protein, 10 mM sodium phosphate, pH 6.5) with a JASCO J-715 CD spectrometer (JASCO Corp.) at 293 K and were analyzed for helical content with the DICHROWEB software (3) using the k2d algorithm (3). The molar ellipticity at 222 nm was measured from 277–368 K (in 1-K intervals), and the data were fit to a simple two-state thermodynamic model of unfolding (4).

NMR Analysis and Structure Determination. Standard NMR experiments for resonance assignments, distance, and torsional angle restraints were measured on a Varian 500 MHz Unity+ spectrometer at 25 °C. Residual dipolar couplings were measured by adding ~4% of PEG:hexanol ($C_{12}E_5$; r = 0.85) (5) to a triple-labeled sample (both p66α- and MBD2-labeled) and $^{1}D_{NH}$, $^{1}D_{NC'}$, and $^{1}D_{HNC'}$ couplings were determined using standard in-phase anti-phase (IPAP)- and transverse relaxation optimized spectroscopy (TROSY)-based experiments (6). The structure of the complex was calculated by simulated annealing using the Xplor-NIH (7) software package. The minimized target function included the experimental NMR restraints [NOE-derived interproton distances, torsion angles restraints from J-coupling measurements and from chemical shifts using TALOS+ (8), and residual dipolar couplings], hydrogen bond distance and angle restraints for α-helical residues [identified based on NH(i)-NH(i+1), NH(i)-Hα(i-3), and Hα(i)-Hβ(i-3) NOEs, backbone torsion angles, and lack of NH-H_2O exchange cross-peaks], quartic van der Waals repulsion term for the nonbonded contacts (9), and a torsion angle database potential of mean force (10).

Cell Culture. Chemical inducer of dimerization (CID)-dependent β-globin yeast artificial chromosome (β-YAC) bone marrow progenitor cells, a kind gift from Kenneth R Peterson (University of Kansas Medical Center, Kansas City, KS), were maintained in Iscove's modified Dulbecco's medium (IMDM) supplemented with 10% heat-inactivated FBS, 50 U/mL penicillin and streptomycin, and 100 nmol/L AP20187 (Ariad Pharmaceuticals) (11). MEL-ρ (12) and 293T cells were maintained in RPMI 1640 medium and DMEM, respectively, containing 10% FBS and 100 U/mL penicillin and streptomycin. All cells were grown at 37 °C and 5% CO_2.

CD34$^+$ Progenitor Isolation and Culture. De-identified 10-mL apheresis packs obtained from the Virginia Commonwealth University Bone Marrow Transplant Laboratory were thawed in a water bath at 37 °C. Cells were diluted with an equal volume of PBS/2% FBS. Then 30 mL of cells were loaded onto 15 mL of Ficoll-Paque Plus (StemCell Technologies) and spun at 400 × *g* for 30 min with no brake. The middle mononuclear layer was extracted, diluted to 40 mL with PBS/2%FBS/1 mM EDTA, and passed through a 70-μM nylon filter. Cells then were spun at 250 × *g* for 6 min at 25 °C, and the pellet was resuspended in 1.5 mL of DNase I and 5 mL of 2% FBS in 1× PBS and incubated at room temperature for 10 min. After the addition of 20 mL of 2% FBS/1× PBS/1 mM EDTA to the suspension, cells were spun at 250 × *g* for 6 min at 25 °C. The pellet then was resuspended in 2 mL of application solution (RoboSep Buffer; StemCell Technologies). The EasySep kit from StemCell Technologies was used for positive selection of CD34$^+$ cells according to the manufacturer's protocol. Before lentiviral infection, cells were maintained in growth medium consisting of StemSpan serum-free expansion medium (SFEM) with 1× CC100 cytokine mix (StemCell Technologies) and 2% Pen Strep (Invitrogen), and the medium was changed every 3 d.

Lentiviral Packaging. The MBD2 shRNA sequence (GGGTAAACCAGACTTGAA) was cloned into the pLVTHM vector and then packaged into a lentiviral vector as following: 1.3 μg/μL pCMV-dR8.74, 1.12 μg/μL pMD2G, and 5.0 μg MBD2 shRNA were transfected into 6 × 10^6 293T cells by calcium phosphate precipitation as previously described. The medium was removed after 16 h, and 9 mL of fresh medium was added, followed by incubation for 24 h before harvesting in freezing medium on dry ice and storage at −80 °C.

Lentiviral Infection and Erythroid Differentiation of CD34$^+$ Cells. CD34$^+$ hematopoietic stem cells (1 × 10^5) were plated in 100 μL of growth medium per well in a 24-well plate. Then 250 μL of lentiviral shRNA and 4 μg/mL of polybrene were added. Cells were incubated at 37 °C, 5% CO_2 in a shaker for 20 h. Growth medium was added, and cells were transferred to a regular incubator at 37 °C, 5% CO_2. Positively infected cells were sorted by flow cytometry by the presence of GFP. CD34$^+$ cells then were differentiated in a medium consisting of StemSpan SFEM with 2% Pen Strep (Invitrogen), 20 ng/mL stem cell factor, 1 U/mL erythropoietin, 5 ng/mL IL-3, 2 μM dexamethasone, and 1 μM estradiol. RNA isolation, quantitative PCR (qPCR), and Western blotting were performed as previously described.

Bisulfite Conversion and Sequencing. Genomic DNA from Mel-ρ cells was isolated using the Aquapure Genomic DNA Isolation Kit (Bio-Rad Laboratories). Bisulfite conversion was performed using Methyl-Detector Kit (Active Motif) according to the manufacturer's protocol. The cytosine-guanosine (CpG) island region between +125 and +376 of the chicken ρ-globin gene was

PCR amplified using methylation-insensitive primers designed using Methyl Primer Express V1.0 (Applied Biosystems): AAG TTT TGG TTA GGT GGG TTT (forward) and CTT CCC CAA AAA AAC TCA AC (reverse). Touchdown PCR conditions with an initial 20 cycles of progressively decreasing annealing temperatures from 62 °C to 52 °C and an additional 30 cycles of PCR with annealing temperature of 52 °C was performed. The PCR products were cloned into pGEM T-Easy Vector (pGEM T-Easy Kit; Promega). Four clones were sequenced and analyzed both for complete conversion and for methylation using Java BiQ Analyzer software package (http://biq-analyzer.bioinf.mpi-sb.mpg.de/) to generate lollipop-style methylation diagrams.

1. Cai M, et al. (2003) Solution structure of the phosphoryl transfer complex between the signal-transducing protein IIAGlucose and the cytoplasmic domain of the glucose transporter IICBGlucose of the Escherichia coli glucose phosphotransferase system. *J Biol Chem* 278:25191–25206.
2. Jason-Moller L, Murphy M, Bruno J (2006) Overview of biacore systems and their applications. *Curr Protoc Protein Sci*, 10.1002/0471140864.ps1913s45.
3. Whitmore L, Wallace BA (2004) DICHROWEB, an online server for protein secondary structure analyses from circular dichroism spectroscopic data. *Nucleic Acids Res* 32(Web Server issue):W668-73.
4. Koepf EK, Petrassi HM, Sudol M, Kelly JW (1999) WW: An isolated three-stranded antiparallel beta-sheet domain that unfolds and refolds reversibly; evidence for a structured hydrophobic cluster in urea and GdnHCl and a disordered thermal unfolded state. *Protein Sci* 8:841–853.
5. Rückert M, Otting G (2000) Alignment of biological macromolecules in novel nonionic liquid crystalline media for NMR experiments. *J Am Chem Soc* 122:7793–7797.
6. Lipsitz RS, Tjandra N (2004) Residual dipolar couplings in NMR structure analysis. *Annu Rev Biophys Biomol Struct* 33:387–413.
7. Schwieters CD, Kuszewski JJ, Tjandra N, Clore GM (2003) The Xplor-NIH NMR molecular structure determination package. *J Magn Reson* 160:65–73.
8. Shen Y, Delaglio F, Cornilescu G, Bax A (2009) TALOS+: A hybrid method for predicting protein backbone torsion angles from NMR chemical shifts. *J Biomol NMR* 44:213–223.
9. Clore GM, Gronenborn AM (1998) New methods of structure refinement for macromolecular structure determination by NMR. *Proc Natl Acad Sci USA* 95: 5891–5898.
10. Clore GM, Kuszewski J (2002) Chi(1) rotamer populations and angles of mobile surface side chains are accurately predicted by a torsion angle database potential of mean force. *J Am Chem Soc* 124:2866–2867.
11. Blau CA, et al. (2005) γ-Globin gene expression in chemical inducer of dimerization (CID)-dependent multipotential cells established from human β-globin locus yeast artificial chromosome (β-YAC) transgenic mice. *J Biol Chem* 280:36642–36647.
12. Kransdorf EP, et al. (2006) MBD2 is a critical component of a methyl cytosine-binding protein complex isolated from primary erythroid cells. *Blood* 108:2836–2845.

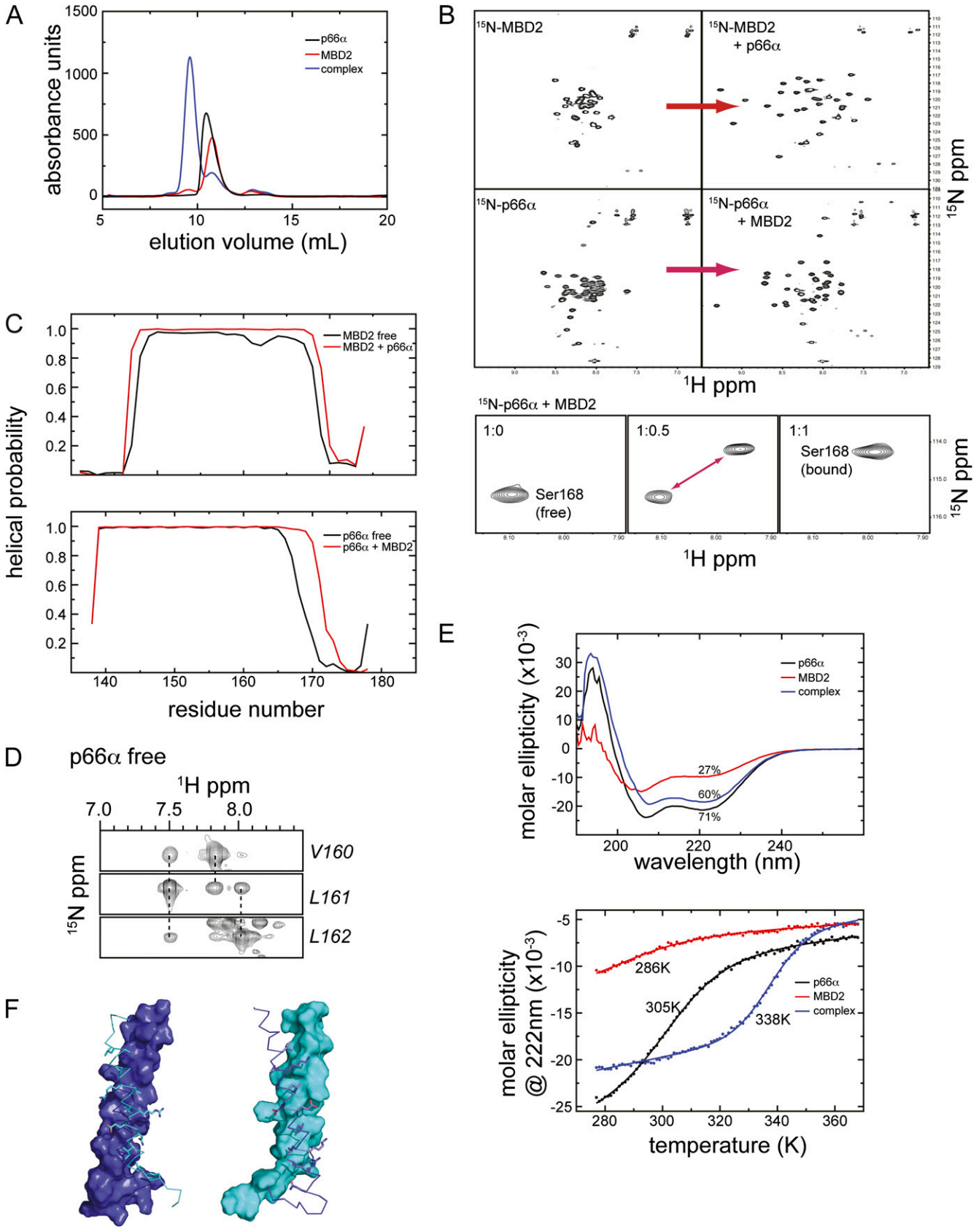

Fig. S1. Binding analyses of the p66α–MBD2 coiled-coil complex. (*A*) Size exclusion chromatography (Superedex75 10/300; GE Healthcare) elution profiles are shown for p66α and MBD2 coiled-coil domains (with N-terminal thioredoxin fusion polypeptides) in isolation and as a 1:1 molar mixture. The mixture elutes as a single peak earlier than either individual protein, consistent with formation of a stable 1:1 complex. (*B*) 2D ^{15}N-heteronuclear single quantum coherence

Legend continued on following page

(HSQC) NMR spectra are shown for ^{15}N-labeled coiled-coil domains free and in complex with unlabeled partners (MBD2 is shown in the upprt two panels, free on the left; p66α is shown in the lower two panels, free on the left). Binding is associated with greater peak dispersion and line broadening. Expanded regions of 2D ^{15}N-HSQC NMR spectra are shown for Ser168 of ^{15}N-p66α at three different molar ratios of unlabeled MBD2 (1:0, 1:0.5, and 1:1). Two distinct peaks for Ser168 (representing bound and free) are present at the 1:0.5 molar ratio consistent with slow exchange between states on the NMR time scale. (*C*) The probability that individual residues adopt helical secondary structure as calculated from NMR chemical shifts with TALOS+ (1) is shown for MBD2 and p66α coiled-coil domains as isolated monomers and in complex with each other. These data are consistent with each protein adopting an α-helical secondary structure in isolation as well as in the complex. (*D*) Representative ^{15}N slices from a 3D ^{15}N-NOESYHSQC spectrum of monomeric p66α are shown for three sequential amino acids (*Val160, Leu161*, and *Leu162*). Strong sequential amide NOE cross-peaks are connected with dashed lines demonstrating a characteristic NOE pattern for α-helices. (*E*) Circular dichroism spectra are shown for the p66α and MBD2 coiled-coiled peptides in isolation and as a complex. Each curve is labeled with the percent helical content as calculated with DICHROWEB software (2) using the k2d algorithm (2). Molar ellipticity at 222 nm as a function of temperature is shown for the p66α and MBD2 coiled-coil in isolation and as a complex. The data for each were fit to a two-state thermodynamic model of unfolding as described by Koepf et al. (3), and the curves were labeled with the resulting melting temperature (T_m). (*F*) Two mixed surface and stick representations of the complex between MBD2 (cyan) and p66α (blue). MBD2 (p66α) is shown as a surface representation, and the backbone and key interacting residues of p66α (MBD2) are shown as a stick representation. The figure was generated using the Pymol program (Delano Scientific LLC).

1. Shen Y, Delaglio F, Cornilescu G, Bax A (2009) TALOS+: A hybrid method for predicting protein backbone torsion angles from NMR chemical shifts. *J Biomol NMR* 44:213–223.
2. Whitmore L, Wallace BA (2004) DICHROWEB, an online server for protein secondary structure analyses from circular dichroism spectroscopic data. *Nucleic Acids Res* 32(Web Server issue):W668-73.
3. Koepf EK, Petrassi HM, Sudol M, Kelly JW (1999) WW: An isolated three-stranded antiparallel beta-sheet domain that unfolds and refolds reversibly; evidence for a structured hydrophobic cluster in urea and GdnHCl and a disordered thermal unfolded state. *Protein Sci* 8:841–853.

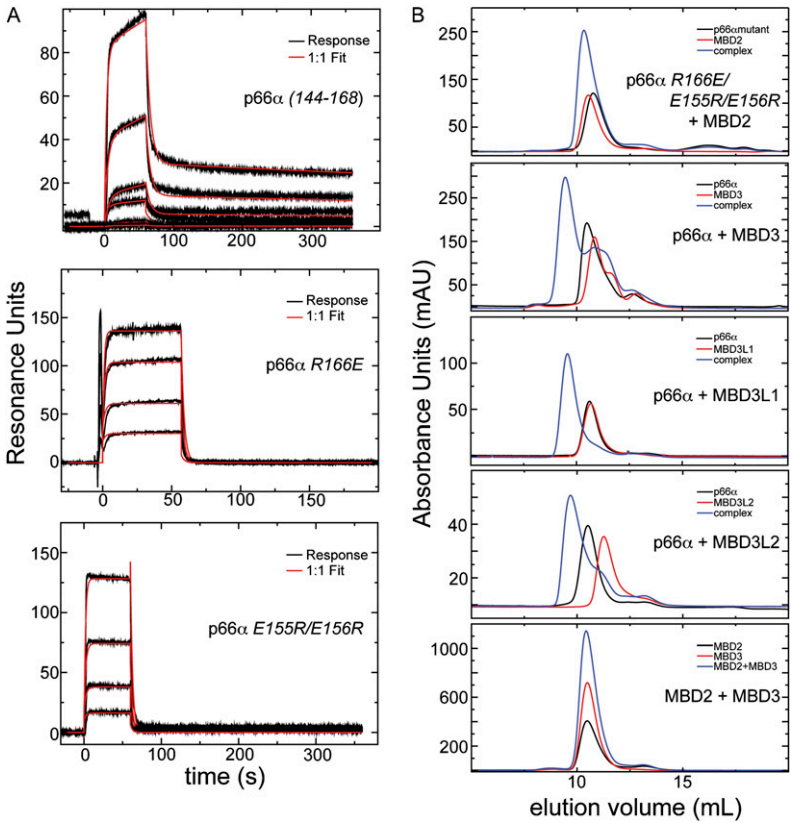

Fig. S2. Coiled-coil domain-binding analysis of p66α mutants and MBD2 homologs. (*A*) Binding kinetics were analyzed for p66α coiled-coil domain truncation (residues 144–168, K_D ~72 nM) and charge mutants (*Arg166Glu* K_D ~8 (M; *Glu155Arg/Glu156Arg* K_D ~ 17 (M) binding to MBD2 coiled-coil coupled to a Sensor Chip CM5 on a Biacore T100 (GE Healthcare). The data were fit to a 1:1 binding model using Biacore evaluation software. (*B*) Size exclusion chromatography elution profiles (Superdex75 10/300) show that the p66α coiled-coil domain *Arg166Glu/Glu155Arg/Glu156Arg* fails to bind the MBD2 coiled-coil domain, but MBD3, MBD3L1, and MBD3L2 coiled-coil domains can form stable complexes with the wild-type p66α coiled-coil domain.

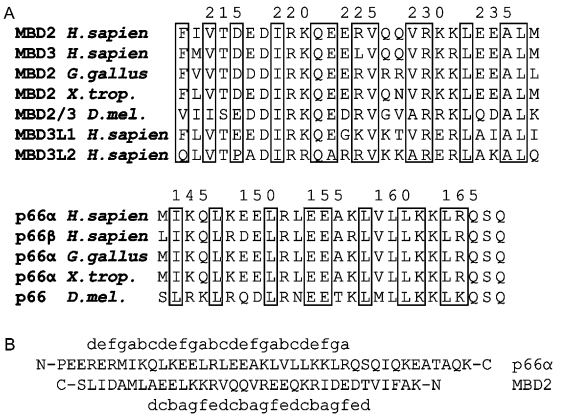

Fig. S3. Key contact residues are highly conserved. (*A*) Alignment of the coiled-coil domain from MBD2 and p66 for different species and for homologous human proteins. Key contacting residues are boxed. (*B*) The anti-parallel heptad repeat is delineated by the letters *a–g* for the p66α and MBD2 coiled-coil regions.

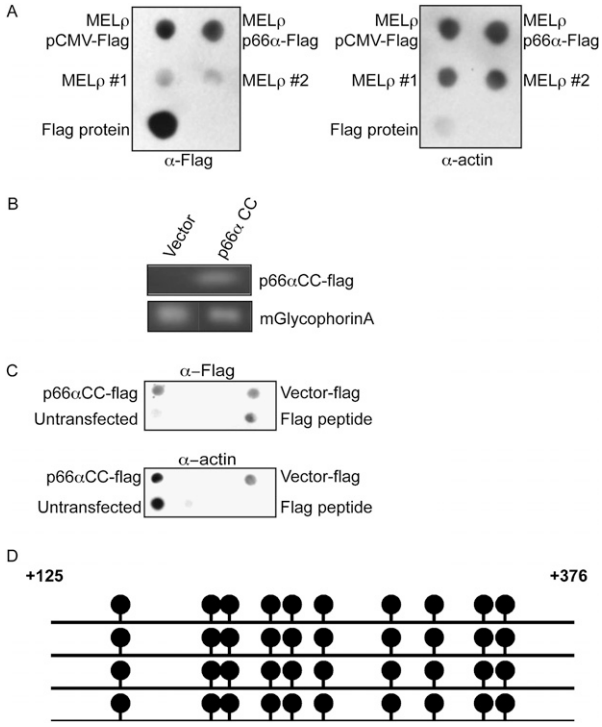

Fig. S4. Protein expression and DNA methylation analysis of p66α-pCMV-Tag2B transfected cells. (*A*) The p66α-pCMV-Tag2B plasmid and an empty vector control were stably transfected into MEL-ρ cells. Dot blot analysis for protein expression (anti-Flag and anti-actin antibodies) shows that both the p66α-pCMV-Tag2B plasmid and empty vector express Flag-tagged peptide, but two different samples of untransfected MEL-ρ cells do not. Purified Flag protein shows appropriate positive reactivity. The p66α-pCMV-Tag2B plasmid and an empty vector control were transiently transfected into CID β-YAC bone marrow progenitor cells. (*B*) RT-PCR analysis using primers specific for Flag-tagged p66α coiled-coil domain cDNA show mRNA expression. (*C*) Dot blot analysis for protein expression (anti-Flag and anti-actin antibodies) shows that both the p66α-pCMV-Tag2B plasmid and empty vector express Flag-tagged peptide, but the untransfected cells do not. (*D*) Bisulfite sequencing of the chicken ρ-globin gene exon1–intron1 CpG island (1) in MEL-ρ cells. Filled circles represent completely methylated CpG sites; open circles represent unmethylated or partially methylated CpG sites (all sites were fully methylated). Each row represents an independent MEL-ρ clone.

1. Singal R, Wang SZ, Sargent T, Zhu SZ, Ginder GD (2002) Methylation of promoter proximal-transcribed sequences of an embryonic globin gene inhibits transcription in primary erythroid cells and promotes formation of a cell type-specific methyl cytosine binding complex. *J Biol Chem* 277:1897–1905.

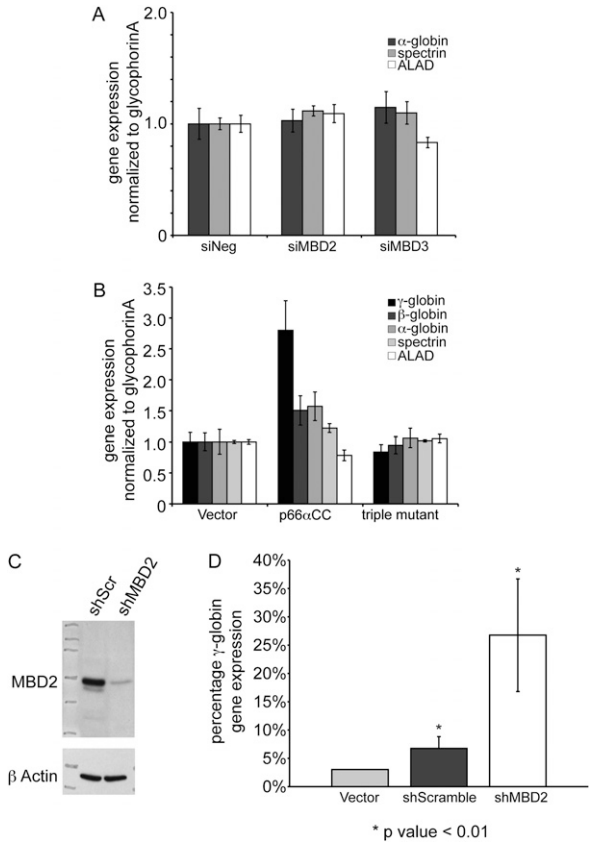

Fig. S5. MBD2 knockdown and p66αCC do not affect the expression of other erythroid-specific genes. (*A*) qPCR analysis shows that knockdown of either MBD2 or MBD3 does not affect mRNA levels of murine α-globin, murine spectrin α1, or murine δ-aminolevulinic acid dehydratase (ALAD). (*B*) qPCR analysis shows that enforced expression of the wild-type or triple-mutant (*Arg166Glu/Glu155Arg/Glu156Arg*) p66α coiled-coil domain does not affect mRNA levels of murine α-globin, murine spectrin α1, murine ALAD, or human β-globin. shRNA knockdown of MBD2 induces γ-globin expression in $CD34^+$ hematopoietic stem cells. (*D*) qPCR analysis shows γ-globin mRNA levels are induced after stable knockdown of MBD2, as shown by Western blotting (*C*). Error bars represent SD.

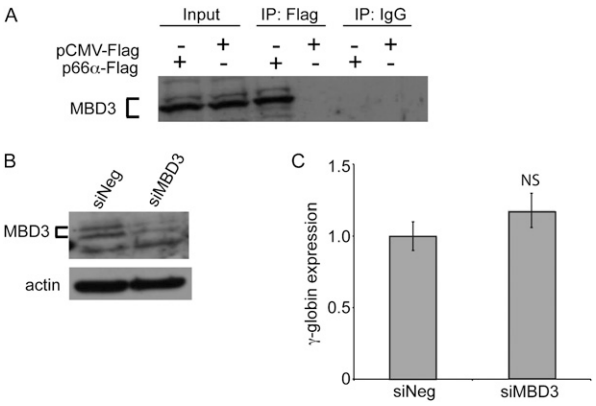

Fig. S6. MBD3 knockdown does not augment γ-globin expression. The p66α-pCMV-Tag2B plasmid and an empty vector control were transiently transfected into high-efficiency 293T cells. (*A*) Immunoprecipitation and Western blot analysis (using anti-Flag and IgG control antibodies) show that native MBD3 co-precipitates with the Flag–p66α coiled-coil domain. (*B*) siNeg and siMBD3 ($n = 3$) were transiently transfected into CID β-YAC bone marrow progenitor cells. Western blot analysis shows efficient knockdown of MBD3 protein. (*C*) qPCR analysis shows that γ-globin mRNA levels were not affected by MBD3 knockdown. Error bars represent SE. NS, not significant.

Table S1. NMR and refinement statistics

NMR distance and dihedral constraints	
Distance constraints	
Total NOE	677
Intraresidue	223
Interresidue	
Sequential ($\|i - j\| = 1$)	203
Medium-range ($\|i - j\| \leq 4$)	145
Long-range ($\|i - j\| > 5$)	0
Intermolecular	106
Hydrogen bonds	94
Total dihedral angle restraints	128
ϕ	58
ψ	58
Total RDCs[‡]	
NH	50
H^NC'	40
NC′	37
Q%	
NH	6.1
H^NC'	30.2
NC′	31.3
Structure statistics	
Violations (mean and s.d.)	
Distance constraints (Å)	0.017 ± 0.004
Dihedral angle constraints (°)	0.27 ± 0.16
Max. dihedral angle violation (°)	3.6
Max. distance constraint violation (Å)	0.39
Deviations from idealized geometry	
Bond lengths (Å)	0.0004 ± 0.00005
Bond angles (°)	0.33 ± 0.0005
Impropers (°)	0.27 ± 0.02
Average pairwise rmsd (Å)	
Heavy	1.2
Backbone	0.5
Ramachandran plot summary[†] (ordered residues)	
Most favored regions	88.4% (98.7%)
Additionally allowed regions	7.0% (1.3%)
Generously allowed regions	3.2% (0.0%)
Disallowed regions	1.4% (0.0%)

*Pairwise rmsd from the mean was calculated among 20 refined structures for ordered residues (p66α: *138–170* ; MBD2: 214–239).
[†]Ramachandran statistics for 20 refined structures for all residues and ordered residues (p66α: *138–170* ; MBD2: 214–239).
[‡]Residual dipolar couplings.

Table S2. Primer sequences

Primers for qRT PCR	Forward primer	Reverse primer	Taqman probe
Human γ-globin	GTG GAA GAT GCT GGA GGA GAA A	TGC CAT GTG CCT TGA CTT TG	FAM/AGG CTC CTG GTT GTC TAC CCA TGG ACC /BHQ
Human β-globin	GCA AGG TGA ACG TGG ATG AAG T	TAA CAG CAT CAG GAG TGG ACA GA	FAM/CA GGC TGC TGG TGG TCT ACC CTT GGA CCC
Chicken ρ-globin	CAG AGG TTC TTT GAT AAC TTC GG	ACG ATG ATG AGG ATG TTC CC	
Murine glycophorin A	GCC GAA TGA CAA AGA AAA GTT CA	TCA ATA GAA CTC AAA GGC ACA CTG T	FAMTTGACATCCAATCTCCTGA GGGTGGTGA /BHQ
Murine MBD2	TTT GAC TTC AGG ACC GGC AAG ATG	ATT GCT CGG GTG GTT CGT GAA TTT	
Murine p66α	AAT AAC GGG TCC TCA CTA CAG	GTA TTC TCG CTG TCG ATC CA	
Murine MBD3	CGC TAT GAT TCT TCC AAC CAG	GTC AAA GGC ACT CAA TCC AC	
Murine Mi2β	GAA CCA CAG GGA GTT AAT GAG	CTT ATA GAG GGA GTA GAG GAA GAC	
p66α- pCMVTag2B	GAT TAC AAG GAT GAC GAC GA	TTT GTA TTT GAC TCT GCC GC	
Murine cyclophilin A	GAG CTG TTT GCA GAC AAA GTT C	CCC TGG CAC ATG AAT CCT GG	FAM/TTC GAG CTC TGA GCA CTG GAG AGA AA/BHQ
Murine spectrin α1	TTA GCA CCA CAT ACA AAC AC	AAA CAT ATC CTT TCC TCC CTG	
Murine ALAD	GAG TTC CCA AGG ATG AAC AG	CTC CTC TGC TAG GAA TGC TC	
Murine α-globin	AAT ATG GAG CTG AAG CCC TGG	ACA TCA AAG TGA GGG AAG TAG GTC T	

Table S3. Antibodies

Antibody	Source
MBD2	Abcam abD-15
MBD2/3	Millipore 07–199
Mi-2	Abcam ab54603, Millipore 06–878
RbAp48	Abcam ab1765
HDAC2	Millipore 05–814
MTA2	Santa Cruz sc-28731
p66	Millipore 07–365

RbAp48, retinoblastoma protein-associated protein 48.